Check for updates

Corresponding Author:
Mangor Pedersen
mangor.pedersen@florey.edu.au

Handling Editor:
Richard Betzel

The MIT Press

RESEARCH

Reducing the influence of intramodular connectivity in participation coefficient

Mangor Pedersen[1], Amir Omidvarnia[1], James M. Shine[2],
Graeme D. Jackson[1,3], and Andrew Zalesky[4]

[1]The Florey Institute of Neuroscience and Mental Health, The University of Melbourne, Melbourne, Victoria, Australia
[2]Brain and Mind Center, The University of Sydney, Sydney, New South Wales, Australia
[3]Department of Neurology, Austin Health, Melbourne, Victoria, Australia
[4]Department of Psychiatry, Melbourne Neuropsychiatry Centre, The University of Melbourne, Victoria, Australia

Keywords: Complex networks, Graph theory, Participation coefficient, fMRI, Airports, *C. elegans*

ABSTRACT

Both natural and engineered networks are often modular. Whether a network node interacts with only nodes from its own module or nodes from multiple modules provides insight into its functional role. The participation coefficient (PC) is typically used to measure this attribute, although its value also depends on the size and connectedness of the module it belongs to and may lead to nonintuitive identification of highly connected nodes. Here, we develop a normalized PC that reduces the influence of intramodular connectivity compared with the conventional PC. Using brain, *C. elegans*, airport, and simulated networks, we show that our measure of participation is not influenced by the size or connectedness of modules, while preserving conceptual and mathematical properties, of the classic formulation of PC. Unlike the conventional PC, we identify London and New York as high participators in the air traffic network and demonstrate stronger associations with working memory in human brain networks, yielding new insights into nodal participation across network modules.

AUTHOR SUMMARY

It is challenging to reliably quantify how single elements (i.e., nodes) in a network are connected to different subcomponents (i.e., modules) of a network; this is important as intermodular connectivity contribute to efficient and distributed information processing. Participation coefficient (PC) calculates how distributed nodes are across modules. But PC is influenced by modularity algorithms that tend to favor large modules with strong intramodule connectivity, that in turn generate low PC values, even if a node has strong intermodule connectivity. We use a network randomization approach and show that by reducing the influence of intramodular connectivity, we obtain node participation results unaffected by size and connectedness of modules. This provides network scientists with new insights into the intermodular connectivity configurations of complex networks.

INTRODUCTION

Many natural and engineered networks are modular. Networks that are highly modular can be partitioned into communities of nodes, or modules, such that the density of connections is greater between the nodes within modules, relative to the density between nodes in different modules. Some nodes have connections that are distributed across many modules, whereas others are only connected with other nodes in their own module. This distinction can provide important insight into a node's functional role in a modular architecture.

Participation coefficient (*PC*): Estimates how well a node within a given module is connected to other brain-wide modules. It is a measure of intermodular diversity.

A node's intermodular connectivity is typically quantified with the participation coefficient (*PC*) (Guimerà & Amaral, 2005). *PC* provides insights into how specific nodes communicate between modules in a range of real-world networks, including air traffic and brain networks (Bertolero, Yeo, Bassett, & D'Esposito, 2018; Guimerà, Mossa, Turtschi, & Amaral, 2005; Kim & Kaiser, 2014; Pedersen, Zalesky, Omidvarnia, & Jackson, 2018; Power, Schlaggar, Lessov-Schlaggar, & Petersen, 2013; Sethi, Pedersen, & Jackson, 2016; Shine et al., 2016; Sohn, Choi, Ahn, Lee, & Jeong, 2011; Towlson, Vértes, Ahnert, Schafer, & Bullmore, 2013). To compute a node's *PC*, the proportion of a node's connections to each module is first determined, yielding a proportion for each module. These proportions are then squared, summed across all modules, and the resulting summand is subtracted from one to yield the node's *PC*. *PC* of zero indicates a node that only connects with other nodes in its own module, whereas nodes with connections that are uniformly distributed across all modules have a *PC* of one.

PC tacitly assumes that all modules in a network are equally sized. This is, however, rarely the case in real-world networks, and nodes in small modules often have high *PC* while nodes in large modules often have low *PC* (Klimm, Borge-Holthoefer, Wessel, Kurths, & Zamora-López, 2014). This is exemplified in the two networks shown in Figure 1, where node *i* in network B, by the virtue of belonging to a larger module, has a lower PC than node *i* in network A, even though node *i* has the same intermodular connectivity in both networks. This toy network example showcases how intramodular connectivity—which is often greater in large modules—influences node participation. This issue was previously addressed by Klimm and others (2014). These authors proposed a dispersion index as well as a novel formulation of *PC*, which adjusts for the effects of intramodular connectivity to address this issue. Their formulation of *PC* involves normalizing intramodular node degrees by module size and then computing the standard deviation across the resulting normalized values. The dispersion index estimates the probability of variance between modular connections. Klimm et al. conceptualize the dispersion index as the relative inability to assign nodes to single modules. In this

A $PC_i = 0.67$ **B** $PC_i = 0.59$
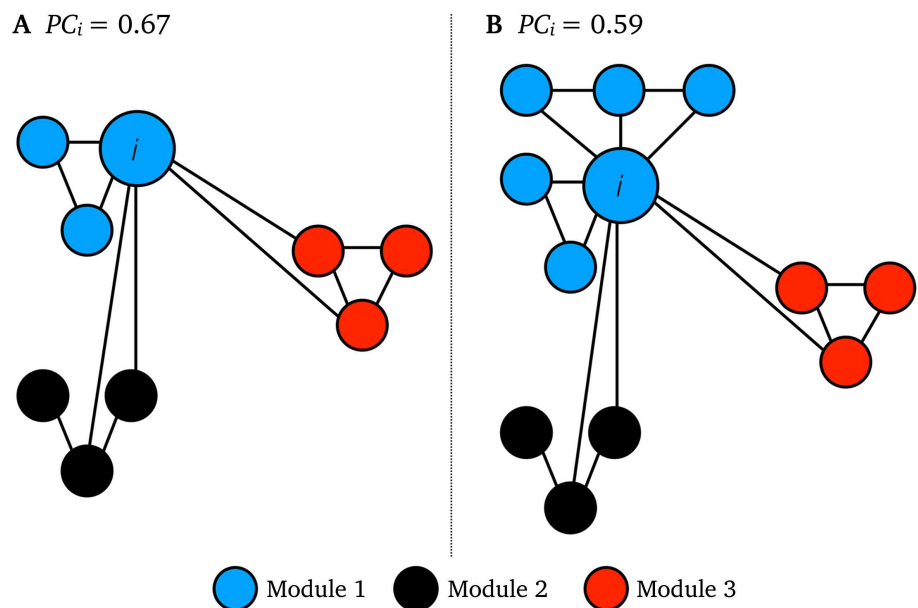
Module 1   Module 2   Module 3

Figure 1. Toy network examples of intramodular connectivity in *PC*. Node *i* has identical intermodular connectivity in network A and B, but it has lower *PC i* in network B as it belongs to a larger blue module than network A.

paper, building on the novel work of Klimm et al., we propose an alternative modification of the *PC* measure that is based on benchmarking intramodular degree using ensembles of numerically-generated null networks. This enables us to quantify the extent to which the intramodular degree of each node is greater than expected under an explicitly formulated null hypothesis. Our aim is to reduce the influence of intramodular connectivity of *PC* while retaining the underlying mathematical assumptions, and numerical range, of the original *PC* measure. To achieve this, we developed a normalized *PC* (PC_{norm}) in which a node's participation is benchmarked to an ensemble of random networks matched in node degree and connection density (Maslov & Sneppen, 2002). PC_{norm} accounts for the intramodular connectivity expected by chance, based on the spatial extent and connectivity pattern of a network's original (i.e., nonrandomized) modules. PC_{norm}, therefore, quantifies a node's intermodular connectivity, while minimizing the influence of the same node's intramodular connectivity. To validate PC_{norm}, we used three real-world networks: (1) undirected functional MRI (fMRI) brain network data with 100 brain regions from 1,003 healthy adults (ages 22–35) participating in the Human Connectome Project (Van Essen et al., 2013); (2) a single directed out-degree network from the *C. elegans* nematode including 277 neurons (Kötter, 2004; White, Southgate, Thomson, & Brenner, 1986); and (3) a single directed out-degree flight network with 500 airports (Marcelino & Kaiser, 2012), as well as simulated networks (Guimerà & Amaral, 2005).

First, simulations were undertaken to test the hypothesis that PC_{norm} preserves the network features and numerical range of *PC*, in networks where all modules were equally sized. We then hypothesized that PC_{norm} would be less correlated with module size—here, we used module size as a proxy intramodular connectivity—than *PC* in real-world networks, across a range of resolution parameters and network density thresholds. In addition to our main hypothesis, we assessed node-specific properties of PC_{norm} to evaluate their relevance in neurobiological and air traffic systems. We also investigated whether PC_{norm} measured in fMRI networks associated with behavior more strongly than *PC*. Together, our results demonstrate a simple refinement of *PC* that retains the interpretation of *PC* in real-world networks but alleviates the effects of intramodular connectivity. Unlike the conventional *PC*, we identify London (LHR) and New York (JFK), among other airports, as high participators in the air traffic network, and demonstrate stronger associations with working memory in human brain networks. We hope PC_{norm} will lead to a more reliable estimation of nodal integration in complex networks.

RESULTS

Normalized Participation Coefficient (PC_{norm})

The participation coefficient (*PC*) measures whether a node interacts with only nodes from its own module or nodes from multiple modules (Guimerà & Amaral, 2005). Formally, the *PC* of node *i* is given by,

$$PC_i = 1 - \sum_{m \epsilon M} \left(\frac{k_i(m)}{k_i} \right)^2,$$

where *M* is the set of network modules, $k_i(m)$ is the degree between node *i*, and all nodes in module *m* and k_i are the degree between node *i* and all other nodes in the entire network. A node with *PC* of zero only interacts with nodes comprising its own module, while nodes with connections uniformly distributed across all modules have a *PC* of one. As first demonstrated and comprehensively addressed elsewhere (Klimm et al., 2014), *PC* is influenced by the extent of intramodular connectivity, which may lead to inaccurate inference in networks with modules that vary in size.

fMRI:
An imaging technique that captures hemodynamic interactions in the brain.

***C. elegans*:**
A nematode with 302 neurons that is approximately 1-mm long.

Gamma resolution parameter:
A parameter that influences the size and extent of network modules.

Network modules:
A collection of network nodes with greater interconnectivity than expected by chance.

To alleviate the effect of intramodular connectivity, we propose the normalized participation coefficient (PC_{norm}),

$$PC_{norm_i} = 1 - \sqrt{B_0 \sum_{m \in M} \left(\frac{k_i(m) - k_i(m)_{rand}}{k_i} \right)^2}.$$

The key difference between PC and PC_{norm} of node i is subtraction of the normalization factor, $k_i(m)_{rand}$, from $k_i(m)$. This normalization factor denotes the median intramodular degree for node i across randomized networks generated with an established network rewiring algorithm that preserves connection density and node degree (i.e., k_i). This also means that k_i is the same for original and randomized networks (Maslov & Sneppen, 2002). We found that 1,000 network randomizations were adequate to return a stable estimate of PC_{norm} (see Supporting Information Figure S1). In each randomized network, all edges were rewired five times. We used the same underlying modular network structure (M) for original $k_i(m)$ and random $k_i(m)_{rand}$. To constrain the range of PC_{norm} between 0 (low network integration) and 1 (high network integration), we add the multiplicative term $B_0 = 0.5$, and we also calculate the square root of the difference of participation between original and randomized networks.

PC and PC_{norm} Are Comparable in Simulated Networks with Equally Sized Modules

First, we aimed to establish that our normalization process does not alter the conceptual basis of the PC. To test this assumption, we implemented the network simulation described by Guimerà and Amral (2005) and verified that PC and PC_{norm} yielded comparable values in a network comprising equally sized modules. Specifically, we simulated binary networks with 100 nodes, and four modules, each containing 25 nodes. We generate networks with a predefined probability of intramodular connectivity (0–1 probability, in increments of 0.01) and intermodular connectivity (0–1 probability, in increments of 0.01), and calculated PC_{norm} (Figure 2A), PC (Figure 2B), and PC_{norm} minus PC (Figure 2C) for all possible connectivity probability values. A single network was generated for each probability value. Given that the modules were equally sized, any intramodular connectivity effects were absent by design, and thus PC and PC_{norm} should not markedly differ.

Figure 2A and 2B suggest that PC_{norm} and PC yield highly comparable estimates across a range of simulated networks with equally sized modules. More specifically, the relationship
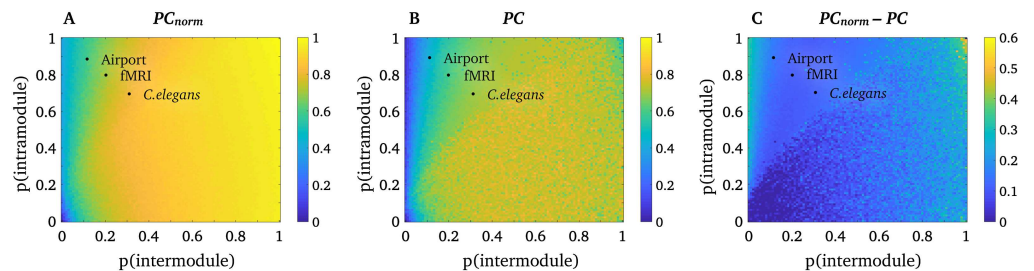

Figure 2. Simulations in networks with equally sized modules. Simulation results for PC_{norm} and PC in networks with equally sized modules, where the heat maps show that average PC across all nodes. (A) PC_{norm} across probabilities of intra- (*y*-axis) and intermodule (*x*-axis) connectivity. (B) PC across probabilities of intra- (*y*-axis) and intermodule (*x*-axis) connectivity. (C) PC_{norm} minus PC across probabilities of intra- (*y*-axis) and intermodule (*x*-axis) connectivity. Black dots represent the proportion of intra- and intermodular connectivity (average of all nodes) of the three real-world networks used in this study.

between PC_{norm} and PC was strong across all simulated networks (Spearman's $\rho^2 = 0.86$). This suggests that PC_{norm} remains consistent with PC in networks with equally sized modules, despite our algorithmic changes to node participation. Our simulation additionally shows that PC_{norm} values reside within the same range as PC (i.e., [0,1]), although PC_{norm} tends to have higher values than PC (see Figures 2, 3, and 8).

PC_{norm} Is Less Correlated with Module Size than PC in Real-World Networks

Next, we aimed to test whether PC_{norm} is less correlated with module size than PC and thus yields more intuitive conclusions about the importance of single nodes in three real-world networks. Using a Louvain modularity decomposition method with a spatial resolution of $\gamma = 1$ (Blondel, Guillaume, Lambiotte, & Lefebvre, 2008), we found that the binary and undirected fMRI human brain networks (number of nodes = 100; network density = 20%) had an average modularity Q-score of 0.35 ± 0.03 [SD] (Q-scores range between 0 and 1 where values proximate to 1 indicate that the network is highly modular, with a predominance of intramodular connections). fMRI human brain networks had an average of 3.52 ± 0.63 [SD] modules, across 1,003 healthy adults. The binary and directed (out-degree) *C. elegans* network (number of nodes = 277; network density = 5.5%) had an average modularity Q-score of
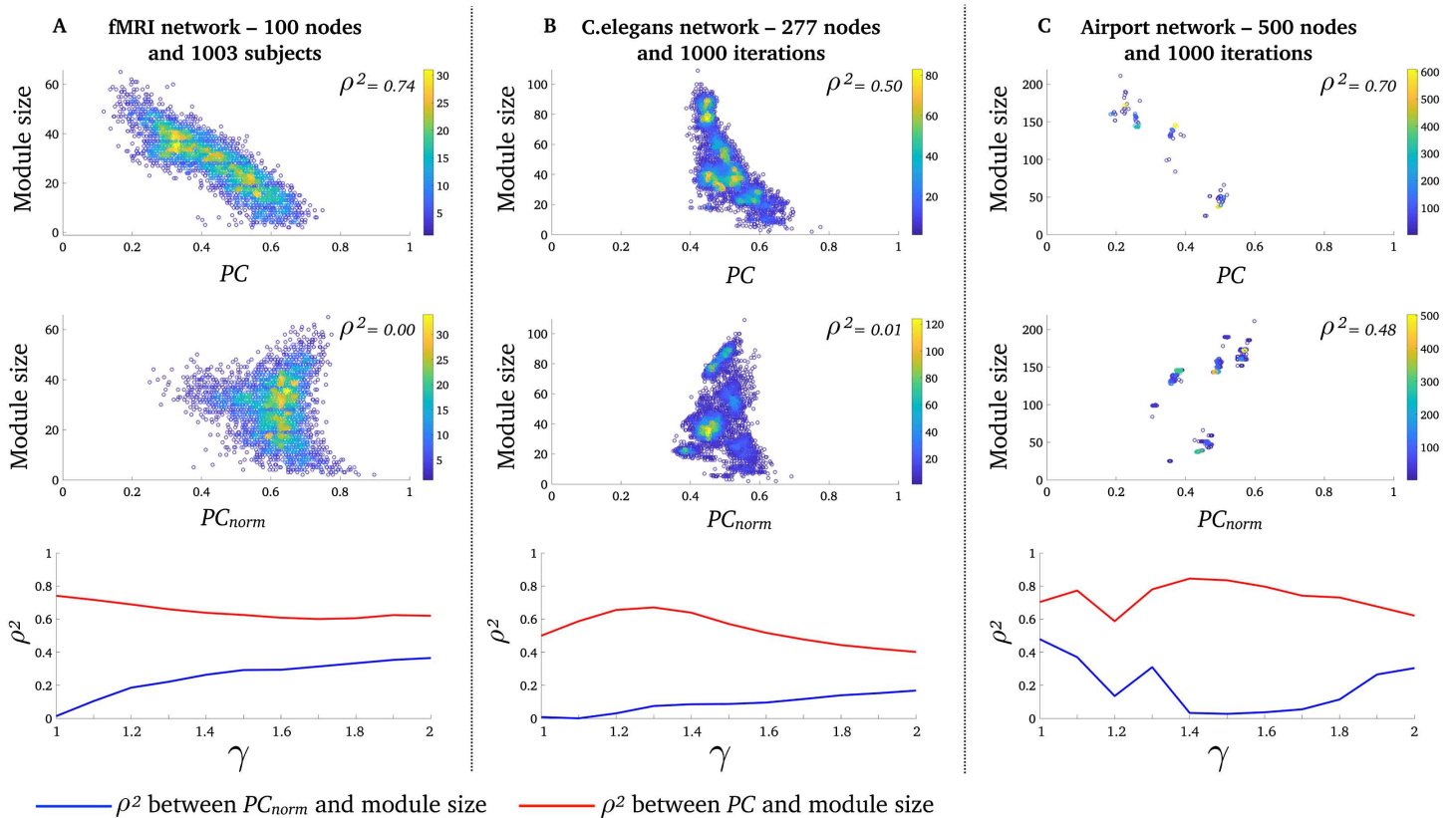

Figure 3. PC_{norm} is less correlated with module size than PC. Relationship between PC and module size (top row), PC_{norm} and module size (middle row), for $\gamma = 1$ (few and large module). Each data point is the average participation of all nodes within a module. Displayed are (A) 3,357 modules (data points) across 1,003 fMRI networks, (B) 6020 modules (data points) across 1,000 *C. elegans* networks, and (C) 3,998 modules (data points) across 1,000 airport networks. Color bars denote the density of overlapping data points. The scatter plots for the airport network appear sparser due to greater consistency across runs of the modular decomposition algorithm relative to the other networks (see Supporting Information Figure S2). The bottom row shows the mean difference between PC, PC_{norm}, and module size for γ between 1 and 2 in 0.1 increments.

0.42 ± 0.01 [SD], and an average of 6.02 ± 0.55 [SD] modules, across 1,000 Louvain modularity iterations. The binary and directed (out-degree) airport network (number of nodes = 500; network density = 19%) had an average modularity Q-score of 0.50 ± 0.01 [SD] and an average of 4.01 ± 0.05 [SD] modules, across 1,000 Louvain modularity iterations (see Supporting Information Figure S3, for results across a range of γ parameters). This resulted in a total of 3,003 networks for analysis, where we for each network calculated the average PC_{norm} and PC across all (nonzero) nodes in each module. We also verified our results across a range of gamma resolution parameters (γ). We included 11 values for the γ-parameters (1 to 2, in increments of 0.1).

To enable statistical inference between the two squared correlation coefficients of interest (correlation value #1 = Spearman's ρ^2 between PC and module size; correlation value #2 = Spearman's ρ^2 between PC_{norm} and module size), we employed a bootstrapping approach using 10,000 bootstrap samples, with replacement (Wilcox, 2016). Here, we aimed to test the null hypothesis of equality in the two correlation coefficients. For each sample, we computed squared correlation coefficients based on the pooled bootstrap samples of participation (PC_{norm} and PC) and module size, as well as its 95% confidence intervals (95% CI).

In line with our hypothesis, we found that the variance explained (ρ^2) between the participation coefficient and module size was substantially lower for PC_{norm} relative to PC (although PC_{norm} and PC were positively correlated in our three real-world networks; see Supporting Information Figure S4), where a module's size was determined by the number of nodes it comprised. This indicates that PC_{norm} reduces the influence of intramodular connectivity compared with PC. We display correlation patterns between PC_{norm}, PC, and module size, in Figure 3, and we summarize the statistical differences between PC_{norm}, PC, and module size in Table 1. It is worth noting there may exist nonmonotonic relationships between PC_{norm} and module size, as Spearman's ρ is unable to detect nonmonotonic correlations.

Given that connection density—that is, the proportion of edges in a network—can markedly impact a network's modular architecture as well as other topological properties (Zalesky et al., 2010), we also confirmed that PC_{norm} reduces the influence of intramodular connectivity compared with PC in fMRI networks, across multiple connection densities (Supporting Information Figure S5). From now on, we report results associated with $\gamma = 1$.

Node-Wise Features of PC_{norm} in Real-World Networks

Next, we investigated the distinct inferences and conclusions that can be reached about the role of specific nodes in our proposed measure of node participation (PC_{norm}). For this purpose, we subtracted average PC from PC_{norm} across 1,003 fMRI network subjects, and 1,000 modularity runs for *C. elegans* and airport networks. In the next few paragraphs we have

Table 1. Mean ρ^2 bootstrap difference, and 95% CI [brackets], with module size between PC and PC_{norm}

	$\gamma = 1$	$\gamma = 1.1$	$\gamma = 1.2$	$\gamma = 1.3$	$\gamma = 1.4$	$\gamma = 1.5$	$\gamma = 1.6$	$\gamma = 1.7$	$\gamma = 1.8$	$\gamma = 1.9$	$\gamma = 2$
fMRI network	0.64	0.35	0.21	0.14	0.09	0.07	0.05	0.03	0.02	0.01	0.01
	[0.55–0.77]	[0.29–0.44]	[0.16–0.27]	[0.12–0.20]	[0.07–0.13]	[0.05–0.09]	[0.04–0.08]	[0.03–0.05]	[0.01–0.02]	[0.01–0.02]	[0.00–0.01]
C.elegans network	0.63	0.56	0.40	0.30	0.26	0.21	0.17	0.12	0.09	0.07	0.05
	[0.52–0.73]	[0.49–0.70]	[0.31–0.47]	[0.21–0.32]	[0.19–0.29]	[0.18–0.28]	[0.14–0.21]	[0.10–0.16]	[0.06–0.10]	[0.05–0.08]	[0.03–0.06]
Airport network	0.22	0.40	0.45	0.47	0.81	0.81	0.76	0.69	0.62	0.41	0.32
	[0.17–0.26]	[0.33–0.44]	[0.38–0.49]	[0.42–0.53]	[0.78–0.82]	[0.77–0.85]	[0.71–0.80]	[0.64–0.75]	[0.56–0.67]	[0.39–0.49]	[0.28–0.36]

summarized node-wise results for fMRI, *C. elegans*, and airport networks. We have also provided a full set of node-wise results for PC_{norm} and PC in Supporting Information Tables S1, S2, and S3, including *z*-score differences between these two measures. A *z*-score was used to calculate the relative differences between PC_{norm} and PC because PC_{norm} tends to yield higher values than PC (Figures 2 and 3). In Supporting Information Figure S6, we display the average modularity structure for fMRI, *C. elegans* and airport networks.

In the brain, the largest difference between PC_{norm} and PC was observed in cerebellum subregions crus I (*z*-score = 1.76), crus II (*z*-score = 1.56), and lobule VI (*z*-score = 1.42), but also in cortical areas such as inferior parietal cortex (*z*-score = 1.31) and superior frontal gyrus (*z* = 1.12) (Figure 4A), areas that are known to connect to a variety of subnetworks in the brain (van den Heuvel & Sporns, 2011) and that subserve higher order cognitive function (Shine et al., 2016). Brain regions with the highest PC_{norm} were cerebellum lobule VI (PC_{norm} = 0.73; PC = 0.49), cerebellum crus I (PC_{norm} = 0.72; PC = 0.46), inferior parietal cortex (PC_{norm} = 0.71; PC = 0.50), middle frontal gyrus (PC_{norm} = 0.71; PC = 0.52), and precuneus (PC_{norm} = 0.70; PC = 0.53) (Supporting Information Table S1).
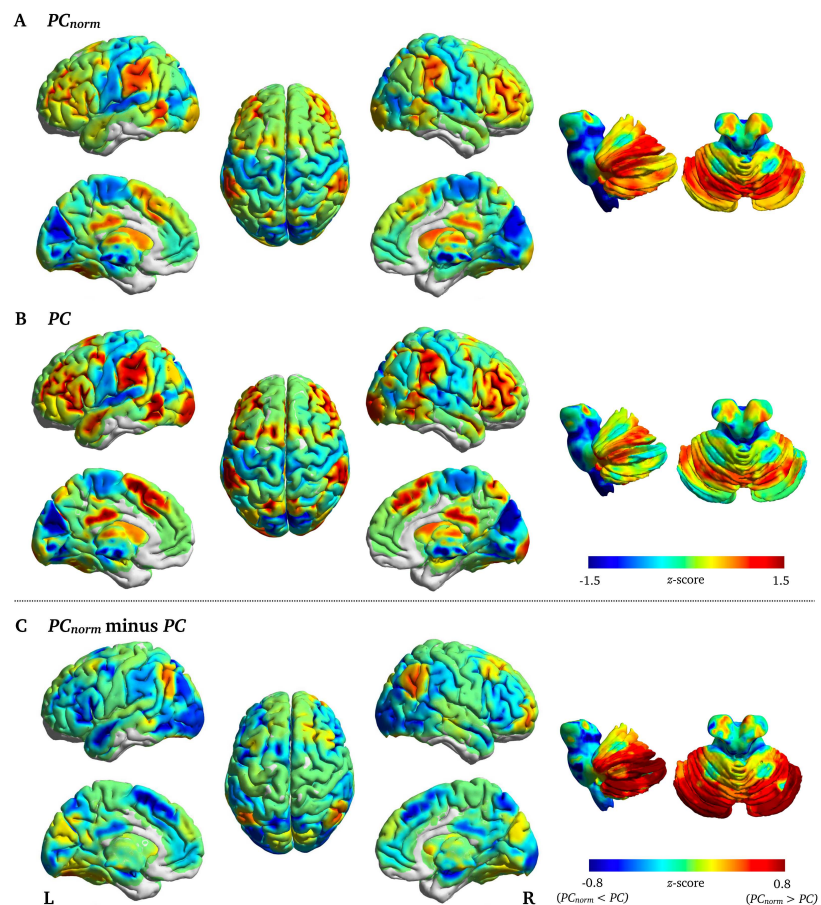

Figure 4. Node-wise fMRI differences between PC_{norm} and PC. Displayed are the subtracted group-average PC from PC_{norm} in fMRI networks (*z*-score). The largest difference between PC_{norm} and PC was observed in cerebellum—subregions lobule VI, crus I, and II—lateral parietal cortex, and insular cortex.
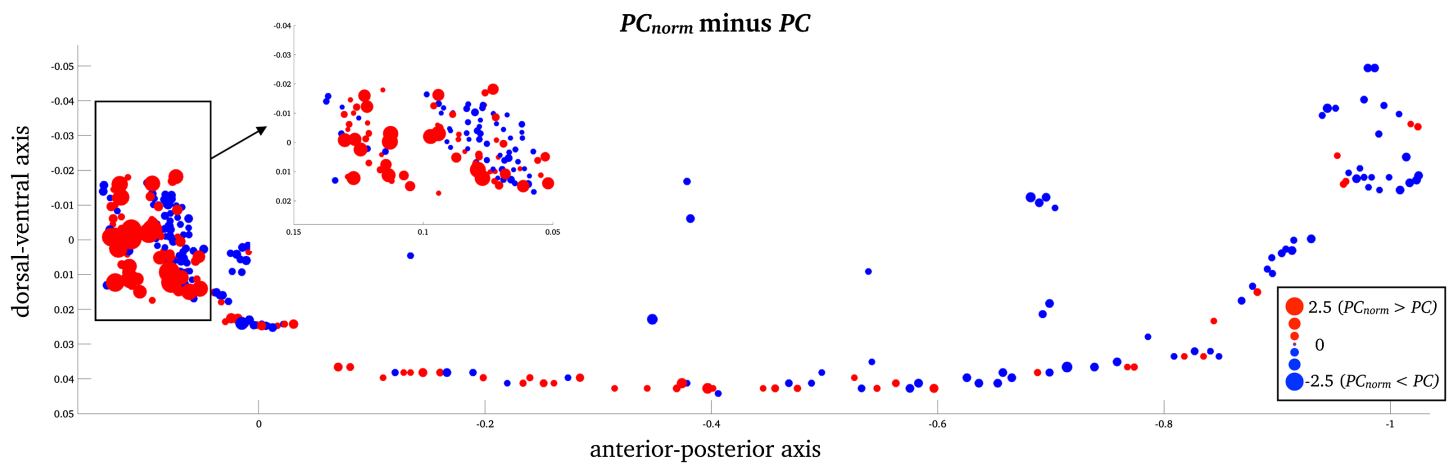
Figure 5. Node-wise *C. elegans* differences between PC_{norm} and PC. Z-score difference between PC and PC_{norm}, in the *C. elegans* network (z-score). The largest difference between PC_{norm} and PC was observed in in inhibitory GABAergic neurons that belong to the largest module of the nematode.

For the *C. elegans* network, the greatest nodal differences between PC_{norm} and PC was observed in the largest module of the nematode encompassing inhibitory GABAergic neurons involved in head movement (RMDDL, z-score = 2.48; RICR, z-score = 2.35; RMDVL, z-score = 2.27; RMDDR, z-score = 2.26; and RMDVR, z-score = 2.23; Figure 5 and Supporting Information Table S2). In the *C. elegans* network, the nodes with greatest difference between PC and PC_{norm} were not among the same nodes that had strongest node participation (PC and PC_{norm}). The strongest PC_{norm} was observed in several interneurons, also located in the head of the nematode including AVER ($PC_{norm} = 0.87$; $PC = 0.75$), AVAR ($PC_{norm} = 0.85$; $PC = 0.75$), AVAL ($PC_{norm} = 0.84$; $PC = 0.75$), AVBR ($PC_{norm} = 0.83$; $PC = 0.74$), and AVBL ($PC_{norm} = 0.80$; $PC = 0.74$), responsible for locomotor behavior, which is an important function for the *C. elegans* nematode. These locomotor interneurons have been found to be densely interconnected across a range of subnetworks forming a selective "rich-club" responsible for a bulk of neural signaling in the nervous system of the *C. elegans* nematode (Arnatkevičiūtė, Fulcher, Pocock, & Fornito, 2018; Bentley et al., 2016; Bertolero, Yeo, & D'Esposito, 2017; Towlson et al., 2013). See https://www.wormatlas.org/neurons/Individual%20Neurons/Neuronframeset.html for full naming, definition, and function of specific *C. elegans* neurons.

In the airport network, the greatest difference between PC_{norm} and PC was observed in South American airports (Montevideo, z-score = −2.26; Sao Paolo, z-score = −2.22; Lima, z-score = −2.20; Rio de Janeiro, z-score = −2.19; and Buenos Aires, z-score = −2.18; see Figure 6A and Supporting Information Table S3), which was the smallest module in this network. Notably, 8 of the 10 airports with highest PC belonged to the module encompassing Central and South America (Figure 6B, red circles). This was in contrast to the nodes with strongest PC_{norm}, which included major airport hubs, including New York-JFK ($PC_{norm} = 0.85$; $PC = 0.61$), Punta Cana ($PC_{norm} = 0.83$; $PC = 0.58$), Toronto ($PC_{norm} = 0.81$; $PC = 0.55$), Montreal ($PC_{norm} = 0.81$; $PC = 0.49$), and Frankfurt ($PC_{norm} = 0.78$; $PC = 0.62$) (see blue circles in Figure 6). These airports are known to have many intercontinental flights. This node-wise analysis suggests that PC overestimates the integrative nature of nodes within relatively small modules and that PC_{norm} can alleviate PC's influence of intramodular connectivity, thereby enabling clearer and more intuitive conclusions to be drawn about the intermodular connectivity of nodes.
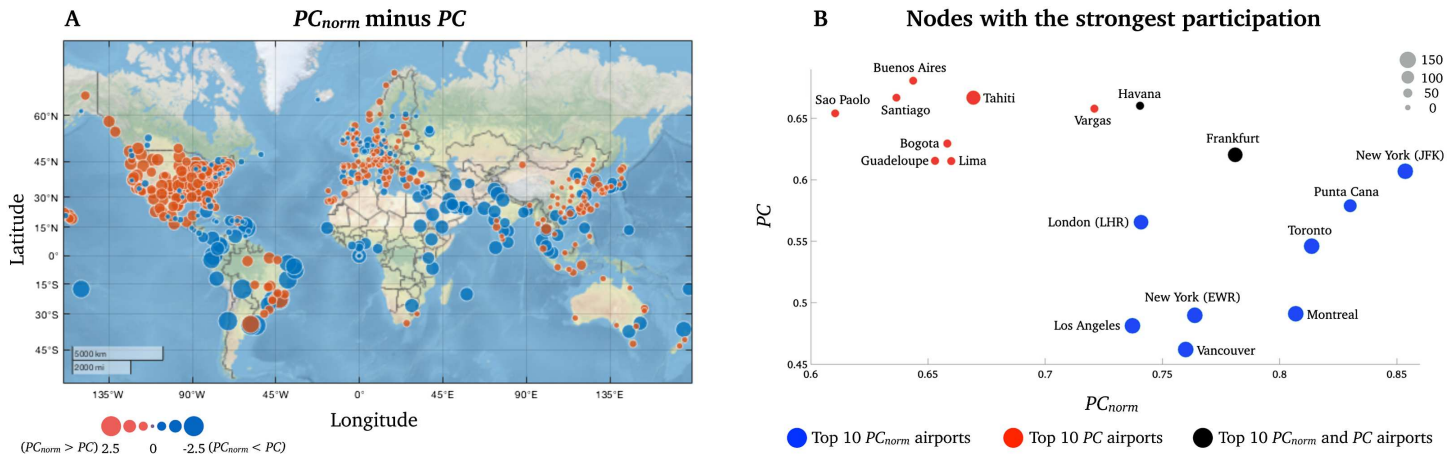
Figure 6. Node-wise difference between PC_{norm} and PC in the network of airports. (A) A world map displaying all airports included in the study. As highlighted in the manuscript, we observed the greatest difference between the two metrics in Central and South American airports (red module). (B) A visual representation of the 10 nodes with strongest PC_{norm} on the *x*-axis (blue nodes) and PC (red nodes) on the *y*-axis. The two black nodes were high for PC_{norm} and PC. Here, the size of each node is proportional to its module size (number of nodes in modules).

PC_{norm} Is More Strongly Correlated with Working Memory Performance than PC

We next aimed to test whether interindividual variation in PC_{norm} measured in brain networks would associate more strongly with behavioral measures than PC (Barch et al., 2013).

We conducted an analysis informed by our previous study where we showed that intermodular network switching was related to the following behavioral domains (Pedersen et al., 2018): (1) *N*-back task, calculated as the average of 0- and 2-back task, important for working memory performance; (2) a relational task central for planning and reasoning; and (3) a sleep index averaging hours of sleep the month before the fMRI scan. Each subject had a single behavioral score for each of the three behavioral domains. We therefore averaged PC_{norm} across all nodes in the network to yield a single PC_{norm} value for each subject. We show that, using the same bootstrapping procedure outlined previously, mean PC_{norm} associated with functional brain networks was correlated more strongly with the *N*-back task compared with PC, but not the sleep index and relational task (Figure 7). This suggests that working memory performance relates to the extent of intermodular connectivity, rather than the size, of modules.

PC_{norm}, PC, and Within-Module Degree Z-Score in Real-World Networks

Within-module degree *z*-score: Normalized degree centrality, i.e., number of links within a module.

PC is often interpreted alongside within-module degree *z*-score, a metric that quantifies the normalized degree of intramodular nodes. First of all, we observed almost no correlation between within-module degree *z*-score and module size (Spearman's $\rho^2 = 0.01$, for γ of 1). We next projected corresponding values between PC and within-module degree *z*-score in a joint histogram which categorizes the intra- and intermodular statuses of nodes (see Figure 8). Similarly to previous work, most network nodes are peripheral nodes classified as nodes that mainly connect to a single module (Guimerà et al., 2005). Note that this definition of peripheral nodes is unrelated to core-periphery networks previously outlined by Csermely, London, and Uzzi (2013). However, our joint histogram analysis showed that PC_{norm} detected more non–hub connector nodes than PC in fMRI networks (Figure 8A). Non–hub connector nodes are classified as nodes that connect to a variety of modules. Airport networks also showed increased PC_{norm} compared with PC, but remained as peripheral nodes (Figure 8B). On the
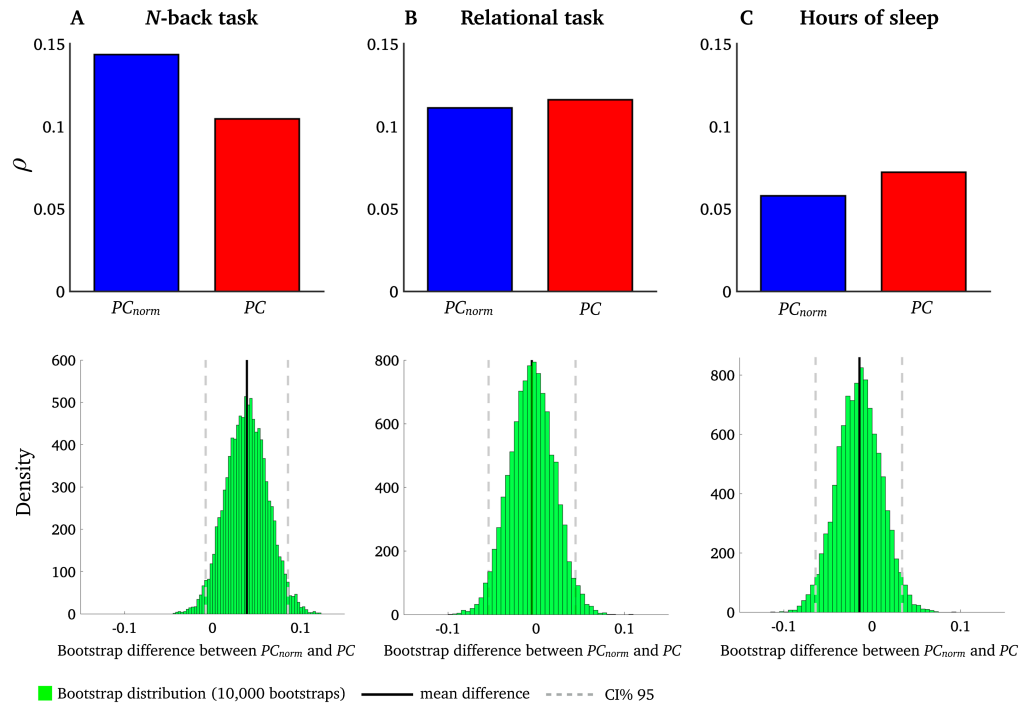
Figure 7. Correlation between PC_{norm}, PC, and behavior. Interindividual variation in PC_{norm} (blue) and PC (red) was associated with three behavioral measures: (A) N-back task, (B) sleep index, and (C) relational task. Spearman's ρ between N-back task and PC_{norm} was 0.14 ($df = 1,001, p < 0.00001$); Spearman's ρ between N-back task and PC was 0.11 ($df = 1,001, p < 0.001$). Bootstrap difference between PC_{norm} and PC for N-back task was 0.04 [95% $CI = -0.01$ to 0.08]. Spearman's ρ between relational task and PC_{norm} was 0.11($df = 1,001, p < 0.001$); Spearman's ρ between relational task and PC was 0.12 ($df = 1,001, p < 0.0001$). Bootstrap difference between PC_{norm} and PC for relational task was 0.01 [95% $CI = -0.05$ to 0.05]. Spearman's ρ between sleep and PC_{norm} was 0.06 ($df = 1,001, p = 0.07$); Spearman's ρ between sleep and PC was 0.07 ($df = 1,001, p = 0.04$). Bootstrap difference between PC_{norm} and PC for sleep was 0.01 [95% $CI = -0.05$ to 0.06].

other hand, PC and PC_{norm} yielded comparable inference about the *C. elegans* network, which primarily comprised peripheral nodes (see Figure 8C). This suggests that PC_{norm} may alter the topological structure, and interpretation, of networks especially in modules of varying sizes.

DISCUSSION

We proposed a normalized participation coefficient (PC_{norm}) to alleviate the effects of intramodular connectivity in the established formulation of PC developed by Guimerà and Amaral (2005). Using brain, *C. elegans*, airport, and simulated networks, we demonstrated that our proposed measure of participation (1) alleviates influence of intramodular connectivity in networks with varying module sizes, (2) preserves the conceptual and mathematical properties of the classic formulation of PC, and (3) yields new insights into the role and function of nodes in the context of their participation across modules, thereby enabling clearer and more intuitive conclusions to be drawn about the role of nodes. Our work should be conceptualized as an extension to Guimerà and Amaral's classic formulation of PC, rather than as a new measure to include in the network scientist's toolbox. We believe PC_{norm} may be useful,
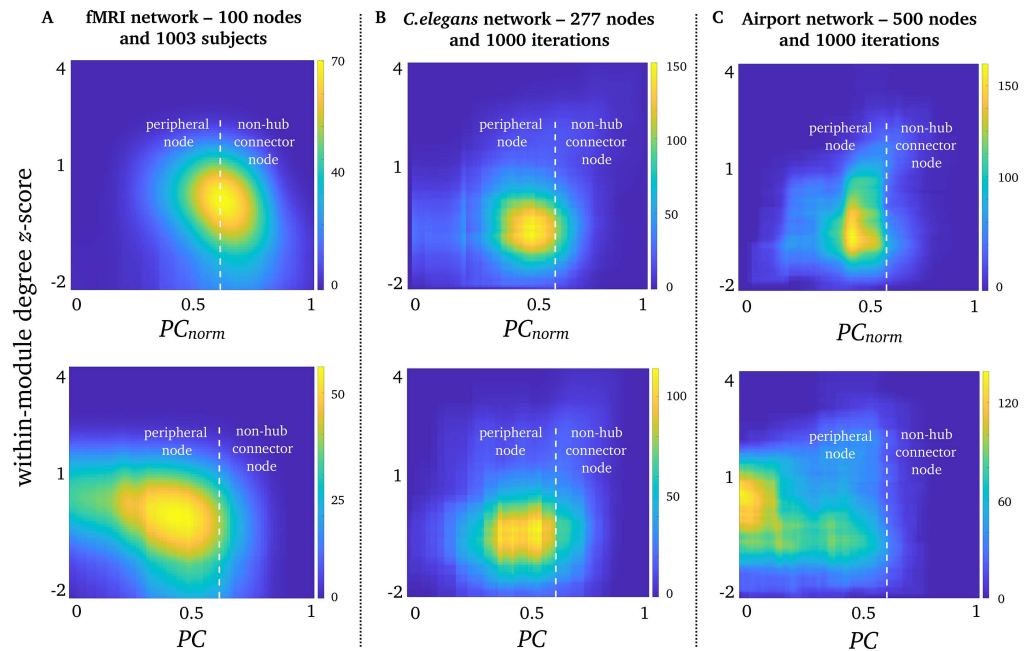
Figure 8. Participation and within-module degree *z*-score. Joint histograms containing the number of simultaneous occurrences between PC_{norm} (top row), PC (bottom row), and within-module degree *z*-score in (A) fMRI networks, (B) *C. elegans* networks, and (C) airport networks. Within-module degree *z*-score is shown on the vertical axis, and PC and PC_{norm} are shown on the horizontal axis. In accordance with Guimerà and Amaral (2005), PC of 0.62 was used to distinguish between peripheral nodes ($PC < 0.62$) and non–hub connector nodes ($PC > 0.62$), and a within-module degree *z*-score < 2.2.

particularly for networks with significant variation in module size. These are the networks for which the intramodular connectivity influences the classic PC.

It is important to clarify and highlight the main reason why we want to reduce the influence of intramodular connectivity in PC, namely network modularity. Modularity decomposition methods are designed to search for a collection of nodes that have stronger and more widespread interconnectedness than we expect by chance (Blondel et al., 2008). Then, a sizable collection of interconnected nodes forming a large module will have low PC values without necessarily reflecting the node's interconnectedness with other modules. An example of this is the case of airport networks. We observed maximal PC in a subset of airports located in the smallest module comprising Central and South America that consequently led to high PC values (Figure 6). After reducing the influence of intramodular connectivity, PC_{norm} suggested that the airports with strongest intermodular connectivity were located in metropolitan cities such as New York, London, and Paris, where over one-third of flights were cross-continental. It is also important to note that PC_{norm}, like PC, appears independent from node degree. This is evident as the two airports with highest PC_{norm} had highly divergent node degree: (1) New York had a total of 218 connections (127 intramodular connections), and (2) Punta Cana in the Dominican Republic had only 52 connections (34 intramodular connections). Although Punta Cana is not a densely connected airport, it belongs to the large module encompassing North America. This airport has a substantial number of cross-continental flights, mainly to South America, again demonstrating how PC may underestimate the integrative nature of nodes within large, and highly intraconnected, modules. It is important for future studies to establish whether these distinct differences between PC_{norm} and PC are generalizable to a range of real-world networks.

An example of the utility of PC_{norm} in real-world networks was seen in fMRI brain networks, where we observed increased intersubject correlation with the *N*-back task compared with *PC* (Figure 7A). This task is important for working memory performance (Kirchner, 1958), a higher order cognitive process that engages a distributed brain network comprising symmetric and bilateral frontal and parietal cortices (LaBar, Gitelman, Parrish, & Mesulam, 1999; Meyer, Spunt, Berkman, Taylor, & Lieberman, 2012). We found that PC_{norm} was relatively high in these regions compared with other areas of the cortex, but this was not as prominent as PC. Several reports also suggest that *PC* is correlated with working memory performance (Bertolero et al., 2018; Cohen & D'Esposito, 2016; Shine et al., 2016; Stanley, Dagenbach, Lyday, Burdette, & Laurienti, 2014). For example, Shine et al. (2016) reported increased *PC* in fronto-parietal networks during the *N*-back task compared with the resting state. This suggests that the human brain may allocate more intermodular connectivity to meet demands of this cognitively strenuous task. Other brain regions that expressed relatively high values of PC_{norm} were located in the cerebellum, mainly subregion Crus I and Lobule VI (see Figure 4A). These cerebellar subregions are also involved in working memory (Desmond & Fiez, 1998; Marvel & Desmond, 2010; Schmahmann & Caplan, 2006). They display connectivity with frontal and parietal cortices (Allen et al., 2005; Bernard et al., 2012) and have preferentially expanded over recent evolutionary time (Shine & Shine, 2014).

Unlike *PC*, nodes that only have intramodular connections will not have a PC_{norm} value of zero. This is because our randomization approach always returns a "random" number to subtract from the original *PC* algorithm. We found that, in real-world networks, PC_{norm} tends to be low when *PC* is zero (Supporting Information Figure S7). However, our simulations showed a difference between PC_{norm} and *PC* in strongly connected nodes in a lattice network (see upper left corner of Figure 2C). This network configuration was not observed in our three real-world networks (see black dots in Figure 2).

Regressing module size from the original *PC* is an alternative to PC_{norm}. This is done by constructing a linear regression model where *PC* of nodes constitute the dependent variable, and the module size associated with each node is the independent variable. Subtracting the fit of the regression model from the original *PC* results in a *residual PC* score. Within this regression framework, a positive residual *PC* score is observed for nodes with participation that is higher than expected because of module size effects alone, whereas negative residual *PC* is observed for nodes with participation that is lower than expected because of module size. Residual PC close to zero indicates that nodes are strongly correlated with module size. Another alternative to PC_{norm} is to exclude intramodular connectivity altogether. This can be achieved by quantifying a node's between-module degree, that is, the number of connections from node *i* to all other nodes that does not belong to node *i*'s module. These additional measures may be useful but require further investigation.

We provide code to calculate PC_{norm}, in addition to residual *PC* and between-module degree, as described in the previous paragraph, available on GitHub (https://github.com/omidvarnia/Dynamic_brain_connectivity_analysis). The current version of PC_{norm} works for undirected/directed and weighted/binary networks. A limitation of PC_{norm} is the computational time needed for network randomizations, which can be particularly time consuming for large networks (i.e., $> 1,000$ nodes). To circumvent this issue, we added a parallel computing option in our code that allows for faster computation time, ensuring this process is tractable for all but the largest networks. Nevertheless, as network randomization procedures are becoming increasingly popular, it is imperative to continue optimizing computational capabilities when randomizing edges in large and complex networks.

METHODS

Modular Decomposition of Networks

Before estimating PC and PC_{norm} (defined in the Results section), we parsed fMRI, *C. elegans*, and airport networks into modules by using a Louvain modularity optimization procedure (Blondel et al., 2008) written as:

$$[Q, M] = \frac{1}{2m} \sum_{ij} \left[A_{ij} - \gamma \frac{k_i k_j}{2m} \right] \delta \left(c_i, c_j \right),$$

where A_{ij} represents the binary connectivity edge between nodes i and j. Louvain modularity optimization procedure finds nodes with greater intramodular connectivity that is expected by chance using a null model where $k_i k_j$ (summation of all edge weights attached to nodes i and j) is divided by $2m$ (m being the summation of all edge weights); c_i and c_j are the modules associated with node i and j, and the module vector output is M; and γ controls the spatial resolution of modules. A low γ ($\gamma < 1.5$) results in a few large modules, whereas a high γ ($\gamma > 1.5$) returns numerous small modules (Bassett et al., 2013). We validated our findings across a variety of γ parameters between 1 and 2 in 0.1 increments, which is a relevant range of gamma values in our networks. The Louvain clustering method also contains heuristics that may cause run-to-run variability due to the degeneracy issue in complex networks (Good, de Montjoye, & Clauset, 2010). This provided us with a good opportunity to assess PC across a range of modular structures in the *C. elegans* and airport network where we only had a single network available for analysis. In these two networks, we obtained 1,000 different modular outputs. In fMRI networks we computed a single modular output of each of the 1,003 subjects by using a consensus clustering approach with 1,000 iterations (Lancichinetti & Fortunato, 2012). For each modularity run in *C. elegans* and airport networks, and fMRI network subject, we obtained a $1 \times N$ vector where N is total number of nodes (i.e., 100 nodes for fMRI networks, 277 nodes for the *C. elegans* neuronal system, and 500 nodes for the airports network) comprising m-numbers of modules (M = all modules).

Within-Module Degree Z-Score

To compare PC and PC_{norm} with intramodular connectivity, we computed within-module degree z-score, that is, the normalized connectivity of a node within its own module (Guimerà & Amaral, 2005). It is given by:

$$z_i = \frac{k_i \left(m_i \right) - \bar{k}(m_i)}{\sigma^{k(m_i)}},$$

where m_i denotes the module containing i, $k_i(m)$ is the overall degree of node i in module m (where node i is located), $\bar{k}\left(m_i \right)$ is the mean degree of all nodes in module m, and $\sigma^{k(m_i)}$ is the standard deviation of all nodes in module m.

Dataset 1: fMRI Network

We used 57.6 min (4,800 time points $\times$ 0.72-s repetition time) of resting-state fMRI data from 1,003 healthy adults between ages of 22 and 35 years, from the Human Connectome Project (Van Essen et al., 2013), that we filtered between frequencies of 0.01 and 0.1 Hz. The fMRI data was distortion, motion, and field bias–corrected and normalized into a common Montreal Neurological Institute space. An independent components analysis was conducted to parcellate the brain into 100 regions of interests (55 subcortical and 45 cortical brain regions). At the

individual level, we generated an undirected binary brain network with 100 nodes by using pair-wise Pearson correlation analysis of subject-specific fMRI time series over 100 brain regions. For our main analysis we thresholded networks at a sparsity level 20% (990 edges). We also derived networks at additional sparsity levels of 10% (495 edges), 30% (1,485 edges), and 40% (1,980 edges; Supporting Information Figure S5).

Dataset 2: C. elegans Network

We analyzed two-dimensional spatial representations of the global neuronal network (277 neurons, or nodes, and 2,105 connections, or edges) of the nematode *C. elegans*, previously identified by electron microscope reconstructions (White et al., 1986). This network is directed and binary, that is, it contains both incoming and outgoing neural connections between brain areas of the *C. elegans*. In this study we only used outgoing connections.

Dataset 3: Airport Network

Airport network was constructed based on flights between the 500 busiest airports (nodes) in the world. Edges were based on the total passenger volume between airports. In this network there were a total of 24,009 flights (edges). The existence of flight connections between airports is based on flights within one year from 1 July 2007 to 30 June 2008 (Marcelino & Kaiser, 2012). An edge means that there is at least one flight between two airports. This network is directed and binary, meaning it contains incoming and outgoing flight connections between airports. In this study we only used outgoing connections.

SUPPORTING INFORMATION

Supporting Information for this article is available at https://doi.org/10.1162/netn_a_00127.

AUTHOR CONTRIBUTIONS

FUNDING INFORMATION

REFERENCES

Allen, G., McColl, R., Barnard, H., Ringe W. K., Fleckenstein, J., & Cullum, C. M. (2005). Magnetic resonance imaging of cerebellar-prefrontal and cerebellar-parietal functional connectivity. *NeuroImage*, *28*(1), 39–48. https://doi.org/10.1016/j.neuroimage.2005.06.013

Arnatkevičiūtė, A., Fulcher, B. D., Pocock, R., & Fornito, A. (2018). Hub connectivity, neuronal diversity, and gene expression in the *Caenorhabditis elegans* connectome. *PLoS Computational Biology*, *14*(2), e1005989. https://doi.org/10.1371/journal.pcbi.1005989

Barch, D. M., Burgess, G. C., Harms, M. P., Petersen, S. E., Schlaggar, B. L., Corbetta, M., . . . WU-Minn HCP Consortium. (2013). Function in the human connectome: task-fMRI and individual differences in behavior. *NeuroImage*, *80*, 169–189. https://doi.org/10.1016/j.neuroimage.2013.05.033

Bassett, D. S., Porter, M. A., Wymbs, N. F., Grafton, S. T., Carlson, J. M., & Mucha, P. J. (2013). Robust detection of dynamic community structure in networks. *Chaos (Woodbury, N.Y.)*, *23*(1), 013142. https://doi.org/10.1063/1.4790830

Bentley, B., Branicky, R., Barnes, C. L., Chew, Y. L., Yemini, E., Bullmore, E. T., . . . Schafer, W. R. (2016). The multilayer connectome of *Caenorhabditis elegans*. *PLoS Computational Biology*, *12*(12), 1–31. https://doi.org/10.1371/journal.pcbi.1005283

Bernard, J. A., Seidler, R. D., Hassevoort, K. M., Benson, B. L., Welsh, R. C., Wiggins, J. L., . . . Peltier, S. J. (2012). Resting state cortico-cerebellar functional connectivity networks: A comparison of anatomical and self-organizing map approaches. *Frontiers in Neuroanatomy*, *6*, 31. https://doi.org/10.3389/fnana.2012.00031

Bertolero, M. A., Yeo, B. T. T., & D'Esposito, M. (2017). The diverse club. *Nature Communications*, *8*(1), 1277–1277. https://doi.org/10.1038/s41467-017-01189-w

Bertolero, M. A., Yeo, B. T. T., Bassett, D. S., & D'Esposito, M. (2018). A mechanistic model of connector hubs, modularity and cognition. *Nature Human Behaviour*, *2*(10), 765. https://doi.org/10.1038/s41562-018-0420-6

Blondel, V. D., Guillaume, J.-L., Lambiotte, R., & Lefebvre, E. (2008). Fast unfolding of communities in large networks. *Journal of Statistical Mechanics: Theory and Experiment*, *2008*(10), P10008. https://doi.org/10.1088/1742-5468/2008/10/P10008

Cohen, J. R., & D'Esposito, M. (2016). The segregation and integration of distinct brain networks and their relationship to cognition. *Journal of Neuroscience*, *36*(48), 12083–12094. https://doi.org/10.1523/JNEUROSCI.2965-15.2016

Csermely, P., London, A., Wu, L.-Y., & Uzzi, B. (2013). Structure and dynamics of core/periphery networks. *Journal of Complex Networks*, *1*(2), 93–123. https://doi.org/10.1093/comnet/cnt016

Desmond, J. E., & Fiez, J. A. (1998). Neuroimaging studies of the cerebellum: language, learning and memory. *Trends in Cognitive Sciences*, *2*(9), 355–362. https://doi.org/10.1016/S1364-6613(98)01211-X

Good, B. H., de Montjoye, Y.-A., & Clauset, A. (2010). Performance of modularity maximization in practical contexts. *Physical Review E*, *81*(4), 046106. https://doi.org/10.1103/PhysRevE.81.046106

Guimerà, R., Mossa, S., Turtschi, A., & Amaral, L. A. N. (2005). The worldwide air transportation network: Anomalous centrality, community structure, and cities' global roles. *Proceedings of the National Academy of Sciences of the United States of America*, *102*(22), 7794–7799. https://doi.org/10.1073/pnas.0407994102

Guimerà, R., & Amaral, L. A. N. (2005). Functional cartography of complex metabolic networks. *Nature*, *433*(7028), 895–900. https://doi.org/10.1038/nature03288

Kim, J. S., & Kaiser, M. (2014). From Caenorhabditis elegans to the human connectome: A specific modular organization increases

metabolic, functional and developmental efficiency. *Philosophical Transactions of the Royal Society B: Biological Sciences*, *369*(1653), 20130529. https://doi.org/10.1098/rstb.2013.0529

Kirchner, W. K. (1958). Age differences in short-term retention of rapidly changing information. *Journal of Experimental Psychology*, *55*(4), 352–358. https://doi.org/10.1037/h0043688

Klimm, F., Borge-Holthoefer, J., Wessel, N., Kurths, J., & Zamora-López, G. (2014). Individual node's contribution to the mesoscale of complex networks. *New Journal of Physics*, *16*(12), 125006. https://doi.org/10.1088/1367-2630/16/12/125006

Kötter, R. (2004). Online retrieval, processing, and visualization of primate connectivity data from the CoCoMac database. *Neuroinformatics*, *2*(2), 127–144. https://doi.org/10.1385/NI:2:2:127

LaBar, K. S., Gitelman, D. R., Parrish, T. B., & Mesulam, M.-M. (1999). Neuroanatomic overlap of working memory and spatial attention networks: A functional MRI comparison within subjects. *NeuroImage*, *10*(6), 695–704. https://doi.org/10.1006/nimg.1999.0503

Lancichinetti, A., & Fortunato, S. (2012). Consensus clustering in complex networks. *Scientific Reports*, *2*, 336. https://doi.org/10.1038/srep00336

Marcelino, J., & Kaiser, M. (2012). Critical paths in a metapopulation model of H1N1: Efficiently delaying influenza spreading through flight cancellation. *PLoS Currents*, *4*, e4f8c9a2e1fca8. https://doi.org/10.1371/4f8c9a2e1fca8

Marvel, C. L., & Desmond, J. E. (2010). Functional topography of the cerebellum in verbal working memory. *Neuropsychology Review*, *20*(3), 271–279. https://doi.org/10.1007/s11065-010-9137-7

Maslov, S., & Sneppen, K. (2002). Specificity and stability in topology of protein networks. *Science (New York, N.Y.)*, *296*(5569), 910–913. https://doi.org/10.1126/science.1065103

Meyer, M. L., Spunt, R. P., Berkman, E. T., Taylor, S. E., & Lieberman, M. D. (2012). Evidence for social working memory from a parametric functional MRI study. *Proceedings of the National Academy of Sciences*, *109*(6), 1883–1888. https://doi.org/10.1073/pnas.1121077109

Pedersen, M., Zalesky, A., Omidvarnia, A., & Jackson, G. D. (2018). Multilayer network switching rate predicts brain performance. *Proceedings of the National Academy of Sciences*, *115*(52), 13376–13381. https://doi.org/10.1073/pnas.1814785115

Power, J. D., Schlaggar, B. L., Lessov-Schlaggar, C. N., & Petersen, S. E. (2013). Evidence for hubs in human functional brain networks. *Neuron*, *79*(4), 798–813. https://doi.org/10.1016/j.neuron.2013.07.035

Schmahmann, J. D., & Caplan, D. (2006). Cognition, emotion and the cerebellum. *Brain*, *129*(2), 290–292. https://doi.org/10.1093/brain/awh729

Sethi, M., Pedersen, M., & Jackson, G. D. (2016). Polymicrogyric cortex may predispose to seizures via abnormal network topology: An fMRI connectomics study. *Epilepsia*, *57*(3), e64–e68. https://doi.org/10.1111/epi.13304

Shine, J. M., & Shine, R. (2014). Delegation to automaticity: The driving force for cognitive evolution? *Frontiers in Neuroscience*, *8*. https://doi.org/10.3389/fnins.2014.00090

Shine, J. M., Bissett, P. G., Bell, P. T., Koyejo, O., Balsters, J. H., Gorgolewski, K. J., . . . , Poldrack, R. A. (2016). The dynamics of

functional brain networks: integrated network states during cognitive task performance. *Neuron*, *92*(2), 544–554. https://doi.org/10.1016/j.neuron.2016.09.018

Sohn, Y., Choi, M.-K., Ahn, Y.-Y., Lee, J., & Jeong, J. (2011). Topological cluster analysis reveals the systemic organization of the *Caenorhabditis elegans* connectome. *PLoS Computational Biology*, *7*(5). https://doi.org/10.1371/journal.pcbi.1001139

Stanley, M. L., Dagenbach, D., Lyday, R. G., Burdette, J. H., & Laurienti, P. J. (2014). Changes in global and regional modularity associated with increasing working memory load. *Frontiers in Human Neuroscience*, 8. https://doi.org/10.3389/fnhum.2014.00954

Towlson, E. K., Vértes, P. E., Ahnert, S. E., Schafer, W. R., & Bullmore, E. T. (2013). The rich club of the *C. elegans* neuronal connectome. *The Journal of Neuroscience*, *33*(15), 6380–6387. https://doi.org/10.1523/JNEUROSCI.3784-12.2013

van den Heuvel, M. P., & Sporns, O. (2011). Rich-club organization of the human connectome. *Journal of Neuroscience*, *31*(44), 15775–15786. https://doi.org/10.1523/JNEUROSCI.3539-11.2011

Van Essen, D. C., Smith, S. M., Barch, D. M., Behrens, T. E. J., Yacoub, E., & Ugurbil, K. (2013). The WU-minn Human Connectome Project: an overview. *NeuroImage*, *80*, 62–79. https://doi.org/10.1016/j.neuroimage.2013.05.041

White, J. G., Southgate, E., Thomson, J. N., & Brenner, S. (1986). The structure of the nervous system of the nematode *Caenorhabditis elegans*. *Philosophical Transactions of the Royal Society B: Biological Sciences*, *314*(1165), 1–340. https://doi.org/10.1098/rstb.1986.0056

Wilcox, R. R. (2016). Comparing dependent robust correlations. *British Journal of Mathematical and Statistical Psychology*, *69*(3), 215–224. https://doi.org/10.1111/bmsp.12069

Zalesky, A., Fornito, A., Harding, I. H., Cocchi, L., Yücel, M., Pantelis, C., & Bullmore, E. T. (2010). Whole-brain anatomical networks: Does the choice of nodes matter? *NeuroImage*, *50*(3), 970–983. https://doi.org/10.1016/j.neuroimage.2009.12.027